APPLIED PHYSICS LETTERS **89**, 132117 (2006)

Origin of forward leakage current in GaN-based light-emitting devices

S. W. Lee,[a] D. C. Oh,[b] H. Goto, J. S. Ha, H. J. Lee, T. Hanada,[c] M. W. Cho,[c] and T. Yao[c]
Center for Interdisciplinary Research, Tohoku University, Aramaki, Aoba-ku, Sendai 980-8578, Japan

S. K. Hong
Department of Materials Science and Engineering, Chungnam National University, Daejeon 305-764, Korea

H. Y. Lee
Faculty of Applied Chemical Engineering, Chonnam National University, 300 Yongbong-dong, Kwangju 500-757, Korea

S. R. Cho, J. W. Choi, J. H. Choi, J. H. Jang, J. E. Shin, and J. S. Lee
LED R&D Laboratory, LG Electronics Institute of Technology, 16 Woomyeon, Seocho, Seoul 137-724, Korea

(Received 26 June 2006; accepted 17 August 2006; published online 28 September 2006)

The authors fabricated GaN-based light-emitting diodes (LEDs) on two different GaN templates with the same LED structure. One on thin GaN template (~2 μm) with high dislocation density [low (10^9 cm^{-2})] grown by metal-organic vapor-phase epitaxy (sample A) and the other on thick GaN template (~20 μm) with comparatively low dislocation density [high (10^8 cm^{-2})] by hydride vapor-phase epitaxy (sample B). In order to understand the mechanism of leakage current in LEDs, the correlation between current-voltage characteristics and etch pit density of LEDs was studied. © *2006 American Institute of Physics*. [DOI: 10.1063/1.2357930]

Leakage current in GaN-based light-emitting diodes (LEDs) is critical for making reliable devices, since it is well correlated with device reliability, lifetime,[1] and degradation in high power operation.[2] Hence the origins of leakage current in electrical characteristics of GaN films have been investigated. Investigation on the reverse-bias current-voltage characteristics of GaN-based LEDs indicated that dislocations with a screw component in GaN films have a strong influence on the reverse leakage current of GaN-based LEDs.[3] The ratio of leakage current of LEDs was found to be about the square of the ratio of density of dislocations with screw dislocations.[4] We would like to mention, however, that most of the studies on leakage current have been conducted on leakage current under reverse-bias conditions, although LEDs are operated under forward-bias conditions. Furthermore, the Shockley equation, generally called diode equation, has been used to analyze the current-voltage (*I-V*) characteristic of *p-n* junctions and Schottky diodes in those diode devices. However, the *I-V* characteristic of LED devices cannot be fully explained by simply applying the Shockley equation, since various parasitic resistances are generated in real devices.[5]

This letter deals with the forward leakage current of GaN-based LEDs to clarify the responsible dislocation types for the forward leakage current.

We fabricated GaN-based light-emitting diodes on two types of GaN templates: one on thin GaN template (~2 μm) with higher dislocation density [low (10^9 cm^{-2})] prepared by metal-organic vapor-phase epitaxy (sample A) and the other on thick GaN template (~20 μm) with comparatively low dislocation density [high (10^8 cm^{-2})] by hydride vapor-phase epitaxy (sample B). The regrowth on the templates to fabricate LED structures was carried out in a vertical metal-organic vapor-phase epitaxy reactor. The LED structure was composed of a Si-doped 3 μm thick *n*-type GaN layer with carrier concentration of 5×10^{18} cm^{-3}, seven period multiple quantum well active layers consisting of 8 nm GaN barriers and 2 nm $In_{0.2}Ga_{0.8}N$ quantum wells, followed by Mg-doped 0.2 μm thick *p*-type GaN layer with carrier concentration of 5×10^{17} cm^{-3}.

To evaluate the density of dislocations, the top *p*-GaN layer of the LED structure was etched in H_2SO_4 for 20 min at 300 °C, and the etched surface was investigated by scanning electron microscopy (SEM) (Hitachi S-4300E). *I-V* measurements were performed with a Hewlett-Packard 4145 semiconductor parameter analyzer.

Figures 1(a)–1(d) show SEM images of etched surfaces of the top *p*-GaN layers of samples A and B. Two types of etch pits are observed with different sizes. The size of a larger size pit is about 30 times larger than that of the most commonly observed pit of 9.2×10^{-7} cm^2. The averaged total etch pit density (EPD) measures 5×10^8 and 2.9×10^8 cm^{-2} for samples A and B, respectively. Large size etch pits are observed in sample A as shown in Figs. 1(a) and 1(d), while there are only a few larger-size pits in sample B as shown in Figs. 1(b) and 1(d). The densities of the larger size etch pit are 1.6×10^6 and 1.4×10^5 cm^{-2} for samples A and B, respectively.

It has been reported that screw and mixed dislocations emerge as smaller-size etch pits, while large-size hexagonal etch pits originate from nanopipes, i.e., open-core screw dislocations.[6] The difference in etch pit size comes from difference in line energy of dislocations.[7,8] This implies that the

---

[a] Author to whom correspondence should be addressed; electronic mail: seogwoo@cir.tohoku.ac.jp

[b] Also at Defense Science & Technology, Hoseo University, Baebang-myeon, Asan-si, Chungcheongnam-do 336–795, Korea.

[c] Also at Institute for Materials Research, Tohoku University, Katahira 2-1-1, Aoba-ku, Sendai 980-8577, Japan.

© 2006 American Institute of Physics
Downloaded 17 Feb 2010 to 130.34.135.83. Redistribution subject to AIP license or copyright; see http://apl.aip.org/apl/copyright.jsp

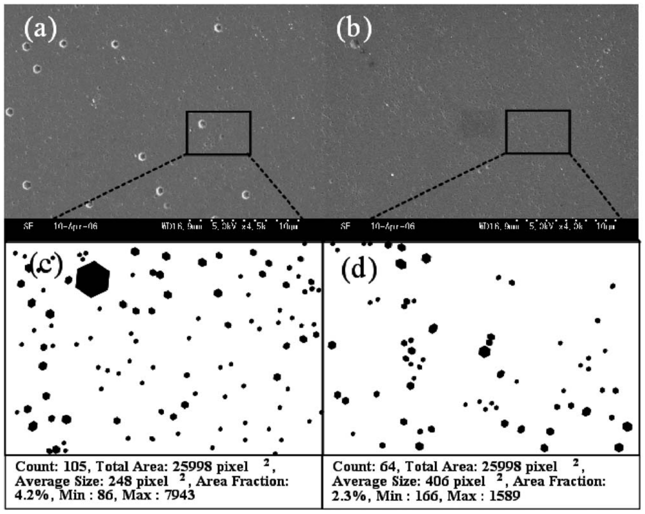

FIG. 1. [(a) and (b)] Typical surface pits of the etched sample A and sample B. [(c) and (d)] Zoomed area to observe in detail. The average EPDs are 5×10^8 and $2.94\times10^8\ \mathrm{cm}^{-2}$ for samples A and B, respectively. Larger size (30 times larger than average pit size) EPDs are 1.6×10^6 and $1.42\times10^5\ \mathrm{cm}^{-2}$ for samples A and B.

line energy of typical nanopipes is larger than the values of a full-core screw and edge dislocation, and that nanopipes are preferentially etched because of their higher line energy. Although the total EPD shows a slight difference for the two samples (only a factor of 2 with more dislocations in sample A than in sample B), sample A shows one order of magnitude larger density of open-core screw dislocation than that in sample B. Nanopipes could be a leakage path of current in GaN-based devices.

Figures 2(a) and 2(b) show *I-V* curves of samples A and B in the forward-biased region. The forward *I-V* curves are replotted in semilogarithmic scale in Fig. 2(b). The *I-V* curves can be clearly divided into three regions: region I for the forward bias voltage less than 2 V, region II for the voltage between 2 and 3 V, and region III for the voltage larger than 3 V. The measured *I-V* characteristics can be understood in the following manner. GaN has extremely low intrinsic carrier concentrations at room temperature: $8\times10^{-11}\ \mathrm{cm}^{-3}$ for electron and $2\times10^{-9}\ \mathrm{cm}^{-3}$ for hole carrier,[9] while carrier concentrations in *p*- and *n*-clad regions are $5\times10^{17}\ \mathrm{cm}^{-3}$ for hole and $5\times10^{18}\ \mathrm{cm}^{-3}$ for electron, respectively. Since carrier concentration in the depletion region is almost zero, the excess current in region I is due to carrier recombination in depletion regions through trap levels presumably associated with threading dislocations (TDs).[10] Region II is well explained in terms of the ideal diode equation for *p-n* junctions assuming diffusion current. A fitting of the ideal diode equation to the experimental data for region II yields ideality factors and saturation current. It should be noted that the two samples have similar ideality factors of ~1.65 and saturation current of 10^{-29} A, indicating that the diode characteristics are essentially the same for the two LEDs within region II. Since *I-V* curves suffer from Ohmic loss by bulk resistance at high bias voltage,[11] the diode current is basically limited by series resistance in *p-/n*-clad regions. The two samples exhibit a similar series resistance of ~90 Ω as shown in Figs. 2(a) and 2(b), which again indicates that the two LEDs are basically the same in terms of electrical characteristics.

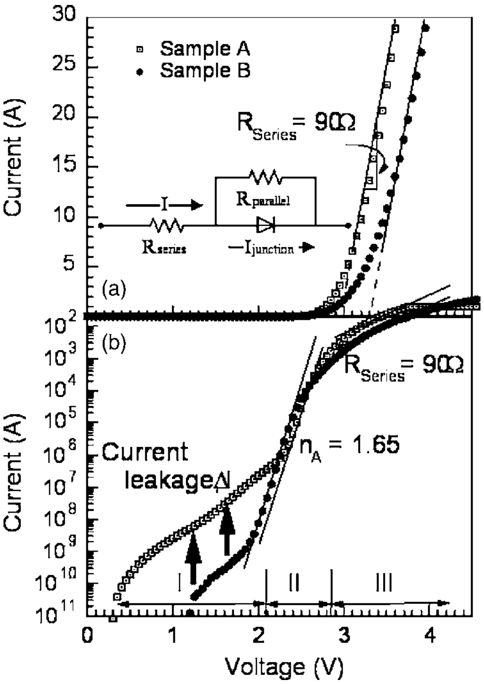

FIG. 2. *I-V* curves for samples A and B in a forward-biased region. (a) Linear scale; inset: the diode circuit model. (b) Log scale.

Although the two LEDs show basically the same electrical characteristics, sample A exhibits larger leakage current (more than two orders of magnitude) than sample B in region I. We have analyzed the observed leakage current taking both ideal diode characteristics and recombination current into account in addition to parallel and series resistances, as shown in the diode circuit model of the inset of Fig. 2(a). *I-V* curves for GaN-based LEDs can be represented by

$$I_{\mathrm{junction}} = I_{\mathrm{diffusion}} + I_{R\text{-}G} = I_{0,A}[\exp(qV/n_A kT) - 1] + I_{0,B}[\exp(qV/n_B kT) - 1], \tag{1}$$

$$\frac{IR_{\mathrm{parellel}} - (V - IR_{\mathrm{series}})}{R_{\mathrm{parallel}}} = I_{\mathrm{junction}}, \tag{2}$$

where I_{junction} is the current that flows across junction, $I_{0,A}$ is the saturation current due to diffusion current, $I_{0,B}$ is the saturation current due to recombination current, n_A is the ideality factor for diffusion current, n_B is the ideality factor for recombination current, q is the unit charge, k is the Boltzmann constant, T is the absolute temperature, I is the total injection current, R_{parallel} is the parallel resistance, and R_{series} is the series resistance.

Figures 3(a)–3(c) show theoretically calculated curves by Eqs. (1) and (2) with variables of R_{paralell}, $i_{0,B}$ and n_B. R_{paralell} can be caused by any paths that bypass the *p-n* junction through TDs. Recombination current is enhanced by the presence of TDs. Hence higher $i_{0,B}$ is expected.[12] The obtained larger n_B values are consistent with the larger recombination current, which is associated with the larger open-core screw dislocation density.[13] It is found that the experimentally obtained *I-V* curves are well fitted by adjusting the three parameters of R_{parallel}, $i_{0,B}$, and n_B, with other parameters being fixed: $I_{0,A}=10^{-29}$ A, $n_A=1.65$, and $R_{\mathrm{series}}=90\ \Omega$ are obtained from the *I-V* characteristics for region II and region III as shown in Fig. 2(b). The experimental *I-V* characteristics of sample B can be well fitted with the calcu-

Downloaded 17 Feb 2010 to 130.34.135.83. Redistribution subject to AIP license or copyright; see http://apl.aip.org/apl/copyright.jsp

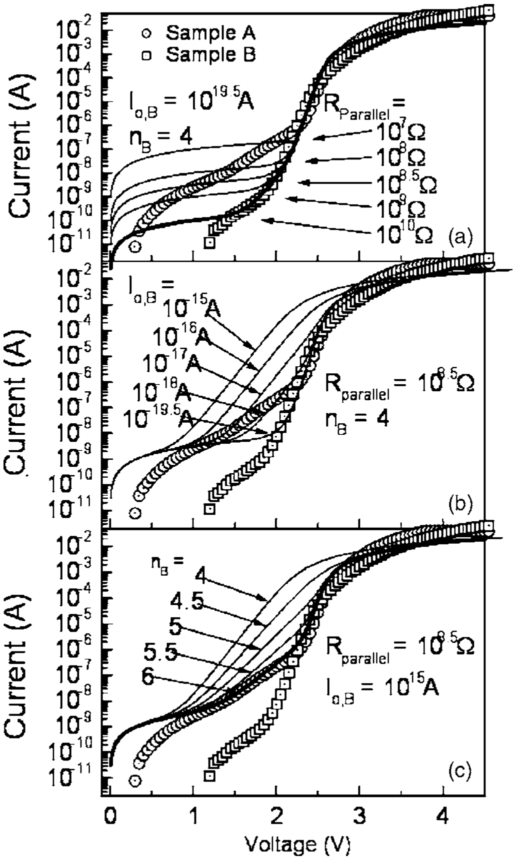

FIG. 3. Theoretically calculated results. (a) Sample B is explained by adopting that $R_{\text{paralell}}=10^{10}\ \Omega$, $I_{0,B}=10^{-19.5}$ A, and $n_B=4$; parallel resistance determines the amount of leakage current; (b) saturation current determines the threshold point that leakage current was rapidly increasesd; (c) ideality factor n_B in a depletion region determines the increase slope of leakage current. Sample A is explained by adopting that $R_{\text{paralell}}=10^{8.5}\ \Omega$, $I_{0,B}=10^{-15}$ A, and $n_B=6$.

lated *I*-*V* curve by adopting $R_{\text{parallel}}=10^{10}\ \Omega$, $I_{0,B}=10^{-19.5}$ A, and $n_B=4$, as shown in Fig. 3(a). The first point we should note is that leakage current is basically determined by parallel resistance as clearly shown in Fig. 3(a). Therefore, the obtained very large parallel resistance of sample B is consistent with the observed small current leakage. The second point is that the crossover between the leakage current (or recombination current) and diffusion current is strongly affected by the saturation current for recombination current, as shown in Fig. 3(b). The obtained extremely small saturation current from curve fitting is consistent with the smaller leakage current for sample B. The third point is that ideality factor n_B is determined by the slope of leakage current as shown in Fig. 3(c). Comparing sample A and sample B, sample A has a larger ideality factor for recombination current than sample B. It is noted that as the leakage current is enhanced, the ideality factor increases and that a large ideality factor is often reported in GaN-based *p*-*n* junction diodes.[14] Contrary to sample B, the *I*-*V* characteristics of sample A can be fitted by decreasing parallel resistance, increasing saturation current, and increasing ideality factor. The *I*-*V* characteristics of sample A are satisfied by adopting $R_{\text{parallel}}=10^{8.5}\ \Omega$, $I_{0,B}=10^{-15}$ A, and $n_B=6$. Comparing sample A and sample B, sample A is much more seriously influenced by larger leakage current.

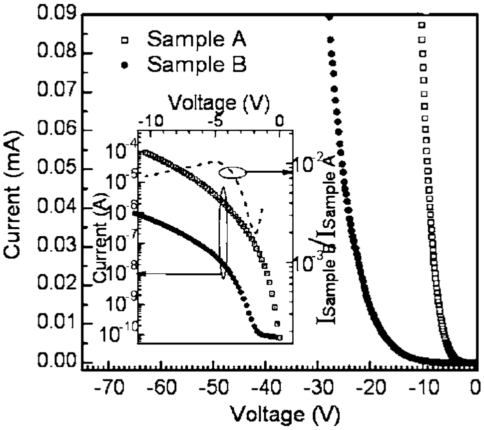

FIG. 4. *I*-*V* curves for samples A and B in a reverse-biased region. Inset: the ratio of leakage current of sample B to that of sample A.

Figure 4 shows *I*-*V* curves for sample A and sample B in the reverse-biase region. We note that sample B has a larger breakdown voltage and smaller reverse-bias current than sample A. The ratio of leakage current of sample B to that of sample A is also shown in the inset of Fig. 4, which is about two orders of magnitude difference. It is reported that the ratio of leakage current of two diodes was proportional to the square of the density of dislocations responsible for leakage current. We note that the ratio of the open-core screw dislocation density for sample A and sample B is about 10, though the total etch pit density is almost the same level for both samples. Hence, it is likely that open-core screw dislocations are responsible for leakage current under the reverse bias. Those considerations lead to the following conclusion: open-core screw dislocations are responsible for leakage current for both forward and reverse biases.

Therefore we have concluded that open-core screw dislocations are responsible for both forward- and reverse-bias leakage currents.

[1] C. H. Liua, R. W. Chuangb, S. J. Changb, Y. K. Sub, L. W. Wub, and C. C. Lin, Mater. Sci. Eng., B **112**, 10 (2004).
[2] X. A. Cao and S. D. Arthur, Appl. Phys. Lett. **85**, 3971 (2004).
[3] J. W. P. Hsu, M. J. Manfra, R. J. Molnar, B. Heying, and J. S. Speck, Appl. Phys. Lett. **81**, 79 (2002).
[4] D. S. Li, H. Chen, H. B. Yu, H. Q. Jia, Q. Huang, and J. M. Zhou, J. Appl. Phys. **96**, 1111 (2004).
[5] *Light-Emitting Diodes*, edited by E. Fred Schubert (Cambridge University Press, Cambridge, 2003), Vol. 1, pp. 55–61.
[6] S. K. Hong, T. Yao, B. J. Kim, S. Y. Yoon, and T. I. Kim, Appl. Phys. Lett. **77**, 82 (2000).
[7] J. Elsner, R. Jones, P. K. Sitch, V. D. Porezag, M. Elstner, Th. Frauenheim, M. I. Heggie, S. Oberg, and P. R. Briddon, Phys. Rev. Lett. **79**, 3672 (1997).
[8] S. K. Hong, B. J. Kim, H. S. Park, Y. Park, S. Y. Yoon, and T. I. Kim, J. Cryst. Growth **191**, 275 (1998).
[9] *Properties of Advanced Semiconductor Materials GaN, AlN, InN, BN, SiC, SiGe*, edited by M. E. Levinshtein, S. L. Rumyantsev, and M. S. Shur (Wiley, New York, 2001), Vol. 1, pp. 1–30.
[10] Z. Z. Bandic, P. M. Bridger, E. C. Piquette, and T. C. McGill, Appl. Phys. Lett. **72**, 3166 (1998).
[11] *The PN Junction Diode, Modular Series on Solid State Devices*, edited by G. W. Neudeck and R. F. Pierret (Addison-Wesley, Reading, MA, 1989), Vol. III, pp. 45–91.
[12] C. L. Andre, D. M. Wilt, A. J. Pitera, M. L. Lee, E. A. Fitzgerald, and S. A. Ringel, J. Appl. Phys. **98**, 014502 (2005).
[13] P. J. Taylor, W. A. Jesser, J. D. Benson, M. Martinka, J. H. Dinan, J. Bradshaw, M. Lara-Taysing, R. P. Leavitt, G. Simonis, W. Chang, W. W. Clark III, and K. A. Bertness, J. Appl. Phys. **89**, 4365 (2000).
[14] *Metal-Semiconductor Contacts*, edited by E. H. Rhoderick and R. H. Williams (Clarendon, Oxford, 1988), Vol. 1, pp. 1–70.

Downloaded 17 Feb 2010 to 130.34.135.83. Redistribution subject to AIP license or copyright; see http://apl.aip.org/apl/copyright.jsp